TECHNICAL MEMORANDUM

241

The ECMWF implementation of three dimensional variational assimilation Part 1: Formulation

P. Courtier, E. Andersson, W. Heckley, J. Pailleux, D.Vasiljević, M. Hamrud, A. Hollingsworth, F. Rabier and M. Fisher

Research Department

January 1998

European Centre for Medium-Range Weather Forecasts
Europäisches Zentrum für mittelfristige Wettervorhersage
Centre européen pour les prévisions météorologiques à moyen

Abstract

In the first of this three-part paper, the formulation of the ECMWF implementation of 3D-Var is described. In the second part, the specification of the structure function is presented, and the last part is devoted to the results of the extensive numerical experimentation programme which was conducted.

The 3D-Var formulation relies on a spherical harmonics expansion in a similar way as the ECMWF OI relied on a Bessel functions expansion. This formulation is introduced using a convolution algebra over the sphere expressed directly in spectral space. It is shown that all features of the OI statistical model can be implemented within 3D-Var. Furthermore a nonseparable statistical model is described. In the present formulation, geostrophy is accounted for through a Hough modes separation of the gravity and Rossby components of the analysis increments. As in OI the tropical analysis remains essentially non divergent and with a weak mass-wind coupling.

The observations used, as well as their specified statistics of errors are presented together with some implementation details.

In the light of the results, 3D-Var was operationally implemented at the end of January 1996.

1 Introduction

Following the presentations at the June 1985 ECMWF workshop on high resolution analysis of the results obtained by Talagrand and Courtier (1987) and Courtier and Talagrand (1987) with a barotropic vorticity equation and the shallow-water results of Courtier and Talagrand (1990), a variational data assimilation project was initiated in 1987 in collaboration between the European Centre for Medium-Range Weather Forecasts (ECMWF) and Météo-France (Pailleux, 1990). Four dimensional variational data assimilation (4D-Var) was foreseen as the ultimate goal, with the three dimensional version (3D-Var) as an important intermediate milestone. 3D-Var was also motivated by the difficulties encountered in the late 80's with the use of retrieved temperature and humidity profiles from the Tiros Operational Vertical Sounder (TOVS) on board the NOAA satellites (see Andersson *et al.* 1991, Kelly *et al.* 1991 and Flobert *et al.* 1991 for a detailed description of these difficulties). This initiated the 1D-Var project of variational retrieval from the TOVS radiances (Eyre, 1989, Eyre and Lorenc, 1989, Thépaut and Moll, 1990) which was implemented operationally in summer 1992 allowing a positive impact of the TOVS data in the Northern Hemisphere (Eyre *et al.* 1993). As described by Andersson *et al.* (1994), 1D-Var was conceived as a pre-processing step of 3D-Var or 4D-Var.

Lorenc (1986) showed that Optimal Interpolation (OI) (see Hollingsworth, 1987 for a thorough description of OI) and 3D-Var are two algorithms for solving the same linear estimation problem. OI has been in operational use at ECMWF since 1979 (Lorenc, 1981, Shaw *et al.* 1987, Undén, 1989). The ECMWF 3D-Var formulation has in many respects been influenced by the experimental work conducted with OI and in particular by the description of the short-range forecast errors of Hollingsworth and Lönnberg (1986) and Lönnberg and Hollingsworth (1986) (referred to as HLLH86 in the following).

Parrish and Derber (1992) and Derber *et al.* (1991) implemented the Spectral Statistical Interpolation analysis scheme (SSI) in June 1991 at the National Centres for Environmental Prediction (NCEP), with recent changes described in Parrish *et al.* (1995). SSI and 3D-Var are very similar variational algorithms. They nevertheless differ in several aspects which will be mentioned during the course of this paper. The UK Meteorological Office (Lorenc, 1995) and the Atmospheric Environment Service (Gauthier *et al.* 1996) are also developing a 3D-Var scheme, the latter being very close to SSI or the ECMWF 3D-Var while the former originally did not make use of the spherical harmonics for representing the statistics of short range forecast errors (Lorenc, 1992). The Data Assimilation Office has devised the PSAS algorithm (Cohn *et al.* 1997) which is in duality with 3D-Var (Courtier, 1997).

This paper describes the formulation of the 3D-Var algorithm. Two companion papers, Rabier *et al.* (1998) and Andersson *et al.* (1998) (referred to as Part II and Part III in the following), describe the calculation of the background error statistics and the experimental results. The extensive experimental programme was followed by operational implementation on 30 January 1996. After this introduction, the second section summarises the 3D-Var principle. The third section presents the background term formulation, the fourth section describes the observations used and the specification of their error statistics. The fifth section summarises some implementation features. Numerical results in idealised cases are followed by a brief conclusion restricted to the formulation aspects. The notations used in the paper follow Ide *et al.* (1997).

2 3D-Var.

In its incremental formulation (Courtier *et al.* 1994), 3D-Var attempts to minimise the objective function J

$$J(\delta\mathbf{x}) = \underbrace{\frac{1}{2}\delta\mathbf{x}^T\mathbf{B}^{-1}\delta\mathbf{x}}_{J_b} + \underbrace{\frac{1}{2}(\mathbf{H}\delta\mathbf{x}-\mathbf{d})^T\mathbf{R}^{-1}(\mathbf{H}\delta\mathbf{x}-\mathbf{d})}_{J_o} \tag{1}$$

$\delta\mathbf{x}$ is the increment and at the minimum the resulting analysis increment $\delta\mathbf{x}^a$ is added to the background $\mathbf{x}^b$ in order to provide the analysis $\mathbf{x}^a$.

$$\mathbf{x}^a = \mathbf{x}^b + \delta\mathbf{x}^a \tag{2}$$

$\mathbf{B}$ is the covariance matrix of background error while $\mathbf{d}$ is the innovation vector

$$\mathbf{d} = \mathbf{y}^o - H\mathbf{x}^b \tag{3}$$

where $\mathbf{y}^o$ is the observation vector. $\mathbf{H}$ is a suitable linear approximation of the observation operator H in the vicinity of $\mathbf{x}^b$, and $\mathbf{R}$ is the covariance matrix of observation errors.

The incremental formulation of 3D-Var consists therefore of solving for $\delta\mathbf{x}$ the inverse problem defined by the (direct) observation operator $\mathbf{H}$, given the innovation vector $\mathbf{d}$. The gradient of J is obtained by differentiating Eq. (1) with respect to $\delta\mathbf{x}$

$$\nabla J = (\mathbf{B}^{-1} + \mathbf{H}^T\mathbf{R}^{-1}\mathbf{H})\delta\mathbf{x} - \mathbf{H}^T\mathbf{R}^{-1}\mathbf{d} \tag{4}$$

At the minimum, the gradient of the objective function vanishes, thus from Eq. (4) we obtain the classical result that minimizing the objective function defined by Eq. (1) is a way of solving (for $\delta\mathbf{x}^a$) the linear system

$$(\mathbf{B}^{-1} + \mathbf{H}^T\mathbf{R}^{-1}\mathbf{H})\delta\mathbf{x}^a = \mathbf{H}^T\mathbf{R}^{-1}\mathbf{d} \tag{5}$$

The solution of 3D-Var also satisfies the OI equation (see e.g. Lorenc, 1986 for this standard result)

$$\delta\mathbf{x}^a = \mathbf{B}\mathbf{H}^T(\mathbf{H}\mathbf{B}\mathbf{H}^T + \mathbf{R})^{-1}\mathbf{d} \tag{6}$$

$\mathbf{HBH}^T$ may therefore be interpreted as the square matrix of the covariances of background errors in observation space while $\mathbf{BH}^T$ is the rectangular matrix of the covariances between the background errors in model space and the background errors in observation space.

Most (if not all) implementations of OI rely on a statistical model for describing $\mathbf{HBH}^T$ and $\mathbf{BH}^T$ (see HLLH86 and Bartello and Mitchell, 1992). 3D-Var uses explicitly the observation operator $\mathbf{H}$ and if, as OI, it requires a statistical model, this is only for describing the statistics of background errors in model space. Consequently it turns out to be easier from an algorithmic point of view to make use in 3D-Var of observations such as TOVS radiances which depend nonlinearly on the basic analysis variables.

3 Formulation of the background term.

In principle, any covariance matrix $\mathbf{B}$ (i.e. positive definite) may be specified in Eq. (1). In operational practice, $\delta\mathbf{x}$ being a vector of size 10^5 to 10^7, $\mathbf{B}$ is a matrix which contains 10^{10} to 10^{14} elements. As a consequence, it is not tractable to deal with any positive definite matrix. Furthermore, as noted by Dee (1995), the available statistical information necessary for specifying the elements of $\mathbf{B}$ is severely limited. All the information useful for the specification of the statistics of a Kalman filter has to be extracted from the sequence of innovation vectors. This corresponds, in operational meteorology, to 10^7 to 10^8 observations per annum and would only allow estimation of several order of magnitude less elements of the $\mathbf{B}$ matrix in order to obtain stable statistics, even relying on some form of ergodicity. A statistical model has therefore to be defined. In the remaining of this section we shall build such a statistical model which incorporates the features observed by HLLH86. The reader is referred to the companion paper Rabier *et al.* (1996) for the actual specification of the statistics.

The J_b formulation is introduced in the following using tensorial analysis since it naturally extends to the infinite dimension case, which considerably simplifies the notations and allows the interpretation with correlation functions. It is possible to present most of the following with matrix notations, see Heckley *et al.* (1993).

3.1 Univariate case, bidimensional.

$\delta\mathbf{x}$ is considered in this subsection as a scalar field defined over the sphere Σ. $\delta\mathbf{x}$ may be decomposed in spherical harmonics Y_n^m

$$\delta \mathbf{x} = \sum_n \sum_{m=-n}^{n} \delta \mathbf{x}_n^m Y_n^m \tag{7}$$

$\delta \mathbf{x}$ is a real field, thus

$$\delta \mathbf{x}_n^m = \delta \mathbf{x}_n^{-m*} = \delta \mathbf{x}_{n_r}^m + \mathbf{i} \delta \mathbf{x}_{n_i}^m$$

where the * denotes the complex conjugate and the subscripts $_i$ and $_r$ indicate respectively the imaginary and real part, and $\mathbf{i}^2 = -1$. The normalisation for the spherical harmonics is the usual one in meteorology

$$\frac{1}{4\pi} \int_\Sigma Y_n^m Y_n^{m*} d\Sigma = 1 \tag{8}$$

Let us consider the random field ξ which we assume unbiased for the sake of simplicity $< \xi >= 0$, $< . >$ standing for the mathematical expectation. We introduce the covariance tensor $\mathbf{T} =< \xi \xi^T >$. A covariance tensor has two entries, and the covariance of two fields x and y is denoted by $\mathbf{T}(x, y)$. If P and Q are two points of the sphere Σ, the covariance between these two points is defined as being $\mathbf{T}(\delta_P, \delta_Q)$, where δ_P and δ_Q are the Dirac distributions at points P and Q respectively. $\mathbf{T}(\delta_P, \delta_P)$ is the variance of the random field ξ at point P. In this section, we assume that the mathematical objects we manipulate are properly defined an finite in the appropriate functional and probabilistic spaces. As an example the variance of any random field ξ is not necessarily well defined, and its existence has some implications on the underlying probability law. This difficulty is discussed to Gaspari and Cohn (1997) and references therein.

3.1.1 Isotropic covariances.

The fundamental result at the heart of 3D-Var (see e.g. Boer, 1983), is that if $\mathbf{T}$ is isotropic, i.e. invariant by all rotations over the sphere, then the spherical harmonics are orthogonal for the metric defined by $\mathbf{T}$, or in other words, the two spherical harmonics fields Y_n^m and $Y_{n'}^{m'*}$ are correlated only if they are equal

$$\mathbf{T}(Y_n^m, Y_{n'}^{m'*}) = \delta_{n-n'} \delta_{m-m'} b_n \tag{9}$$

the modal variance b_n being independent of the zonal wave number m. $\delta_{n-n'}$ is the Kronecker symbol, equal to 1 if $n = n'$ and 0 otherwise. The result is an immediate consequence of the fact that the spherical harmonics provide an irreducible representation of the rotation group of the sphere. Boer (1983) presents an elementary proof which relies on the addition theorem of the zonal spherical harmonics. This proof, sketched below, is by construction and provides an interpretation of the b_n. As $\mathbf{T}$ is isotropic, the covariance between two points P and Q of the sphere is a function of their distance over the sphere only, and therefore of their angular separation θ.

$$\mathbf{T}(\delta_P, \delta_Q) = f(\theta) \tag{10}$$

f may be decomposed in terms of the zonal spherical harmonics $Y_n^0 = P_n^0$.

$$f(\theta) = \sum_n f_n P_n^0(\cos\theta) \tag{11}$$

The Legendre polynomials P_n^0 are normalised and from Eq. (8), one immediately finds

$$\frac{1}{2}\int_0^{\pi} P_n^0(\cos\theta)^2 d\cos\theta = 1 \tag{12}$$

this is why we keep the superscript 0, to distinguish between the normalisation commonly used in mathematics $P_n(1) = 1$, and the normalization used here which implies $P_n^0(1) = \sqrt{2n+1}$.

The addition theorem for the zonal spherical harmonics relates b_n to f_n (Boer, 1983, Courtier, 1987, Wunsch and Stammer, 1995)

$$f_n = b_n\sqrt{2n+1} \tag{13}$$

The variance at any point P is then

$$\begin{aligned}\mathbf{T}(\delta_P, \delta_P) = f(0) = \sum_n f_n P_n^0(1) &= \sum_n f_n\sqrt{2n+1} \\ &= \sum_n b_n(2n+1)\end{aligned} \tag{14}$$

thus b_n is the modal variance while $(2n+1)b_n$ is the total variance for a given total wave number n, and thus provides the power spectrum.

The metric defined by Eq. (8) allows identification of $\mathbf{T}(\bullet, \delta\mathbf{x})$ with a field which may be interpreted as the convolution of the field $\delta\mathbf{x}$ with the isotropic field centered at the northern pole, therefore zonally uniform field, which has the value $f(\theta)$ for a given colatitude θ (see Gaspari and Cohn, 1997 or Yaglom, 1987). Denoting with $*$ the convolution, the addition theorem for the zonal spherical harmonic provides the result

$$(f * \delta\mathbf{x})_n^m = (\mathbf{T}(\bullet, \delta\mathbf{x}))_n^m = \frac{1}{\sqrt{2n+1}}\delta\mathbf{x}_n^m f_n \tag{15}$$

f is said to *represent* the isotropic covariance tensor $\mathbf{T}$ (Gaspari and Cohn, 1997). Since the f_n may be interpreted as a variance, they are necessarily positive. Conversely, any function f with positive Legendre expansion coefficients is the representation of a covariance tensor. This is the Böchner-Schwartz theorem (Gel'Fand and Vilenkin, 1964 p157) in the particular case of the sphere. Let us consider another isotropic tensor $\mathbf{U}$, represented by a function g. Equation (15) applied twice allows definition of the tensor $\mathbf{U} \times \mathbf{T} = \mathbf{T} \times \mathbf{U}$ which is represented by the function $f * g$ with

$$(f * g)_n = \frac{1}{\sqrt{2n+1}} f_n g_n \tag{16}$$

$(\mathbf{U} \times \mathbf{T})(\bullet, \delta\mathbf{x})$ is identified to the field which may be obtained as the convolution of the field $\delta\mathbf{x}$ first with the zonally uniform field which has for a given colatitude θ, $f(\theta)$ for value and then with the zonally uniform field which has $g(\theta)$ for value.

The Dirac distribution at the Northern Pole $\delta_{\mathcal{N}}$ has the following spherical harmonic expansion

$$\begin{aligned} \delta_{\mathcal{N}}{}_n^m = \frac{1}{4\pi}\int_\Sigma \delta_{\mathcal{N}}{}_n^m Y_n^{m*} d\Sigma &= \delta_{m-0} P_n^0(0) \\ &= \delta_{m-0}\sqrt{2n+1} \end{aligned} \tag{17}$$

¿From eq.16 and eq.17, one finds the classical result that the Dirac distribution at the Northern Pole $\delta_{\mathcal{N}}$ is the neutral element of the convolution. Define the inverse of the isotropic covariance tensor $\mathbf{T}$ represented by f as the isotropic tensor denoted by $\mathbf{T}^{-1}$ and represented by a function g such that $f * g = \delta_{\mathcal{N}}$. Combining eq.16 and eq.17, one finds

$$g_n = \frac{2n+1}{f_n} \tag{18}$$

and then

$$(\mathbf{T}^{-1}(\bullet, \delta\mathbf{x}))_n^m = (g * \delta\mathbf{x})_n^m = \frac{\sqrt{2n+1}}{f_n}\delta\mathbf{x}_n^m \tag{19}$$

The expression of J_b immediately follows

$$\begin{aligned} J_b(\delta\mathbf{x}) = \frac{1}{2}\mathbf{T}^{-1}(\delta\mathbf{x}, \delta\mathbf{x}) &= \frac{1}{2}\frac{1}{4\pi}\int_\Sigma \delta\mathbf{x}\mathbf{T}^{-1}(\bullet, \delta\mathbf{x}) d\Sigma \\ &= \frac{1}{2}\sum_n \sum_{m=-n}^{n} \delta\mathbf{x}_n^m \delta\mathbf{x}_n^{m*} \frac{\sqrt{2n+1}}{f_n} \\ &= \frac{1}{2}\sum_n \sum_{m=-n}^{n} \delta\mathbf{x}_n^m \delta\mathbf{x}_n^{m*} \frac{1}{b_n} \\ &= \frac{1}{2}\sum_n \frac{1}{b_n}\left\{\delta\mathbf{x}_n^{0^2} + 2\sum_{m=1}^{n}\left(\delta\mathbf{x}_{n_r}^{m^2} + \delta\mathbf{x}_{n_i}^{m^2}\right)\right\} \end{aligned} \tag{20}$$

Following Daley (1991), the length scale L_s of the isotropic covariance tensor may be defined as

$$L_s^2 = -2\frac{f(0)}{\Delta f(0)} = 2a^2 \frac{\sum_n f_n\sqrt{2n+1}}{\sum_n f_n n(n+1)\sqrt{2n+1}} \tag{21}$$

Δ being the Laplacian operator and a the radius of the sphere Σ.

3.1.2 Preconditioning

In practice, it is necessary to precondition the minimization problem in order to obtain a quick convergence. As the Hessian of the objective function is not accessible, Lorenc (1988) suggested the use of the Hessian of the background term J_b. In practice such a preconditioning may be implemented either by a change of metric in the space of the control variable, or by a change of control variable. As the minimization algorithms have generally to evaluate several inner products, it was found more efficient to implement a change of variable. Algebraically, this requires the introduction of a variable $\mathbf{z}$ such that

$$J_b = \frac{1}{2}\mathbf{z}^T\mathbf{z} \tag{22}$$

Comparing Eq. (1) and Eq. (22) shows that $\mathbf{z} = \mathbf{B}^{-\frac{1}{2}}\delta\mathbf{x}$ would satisfy the requirement. This procedure may directly be applied to Eq. (20), nevertheless, we shall introduce in the following the square root of an isotropic covariance tensor, denoted by $\mathbf{T}^{\frac{1}{2}}$ since this provides an interpretation which will be of some use later. We aim at finding the representation h of $\mathbf{T}^{\frac{1}{2}}$ such that $h * h = f$.

$$(h*h)_n = \frac{1}{\sqrt{2n+1}}h_n^2 \tag{23}$$

which implies

$$(f^{\frac{1}{2}})_n = \quad h_n \quad = \sqrt{\sqrt{2n+1}f_n} \tag{24}$$

$$(f^{-\frac{1}{2}})_n = \quad (h^{-1})_n \quad = \frac{(2n+1)^{\frac{3}{4}}}{\sqrt{f_n}} \tag{25}$$

Introducing $\mathbf{z} = \mathbf{T}^{-\frac{1}{2}}(\bullet, \delta\mathbf{x})$, one finds the expression of J_b

$$\begin{aligned} J_b &= \frac{1}{2}\frac{1}{4\pi}\int_\Sigma \delta\mathbf{x}\mathbf{T}^{-1}(\bullet,\delta\mathbf{x})d\Sigma \\ &= \frac{1}{2}\sum_n\sum_{m=-n}^{n}\delta\mathbf{x}_n^m\delta\mathbf{x}_n^{m*}\frac{\sqrt{2n+1}}{f_n} \\ &= \frac{1}{2}\sum_n\sum_{m=-n}^{n}\left(\frac{1}{\sqrt{2n+1}}\frac{(2n+1)^{\frac{3}{4}}}{\sqrt{f_n}}\delta\mathbf{x}_n^m\right)\left(\frac{1}{\sqrt{2n+1}}\frac{(2n+1)^{\frac{3}{4}}}{\sqrt{f_n}}\delta\mathbf{x}_n^m\right)^* \\ &= \frac{1}{2}\frac{1}{4\pi}\int_\Sigma \mathbf{T}^{-\frac{1}{2}}(\bullet,\delta\mathbf{x})\mathbf{T}^{-\frac{1}{2}}(\bullet,\delta\mathbf{x})d\Sigma \\ &= \frac{1}{2}\frac{1}{4\pi}\int_\Sigma \mathbf{z}^2 d\Sigma \end{aligned} \tag{26}$$

Lorenc(1995) describes a 3D-Var system which makes use of recursive filters to evaluate in grid point space the convolution of $\mathbf{z}$ by $\mathbf{T}^{\frac{1}{2}}$, which is the only convolution necessary to recover $\delta\mathbf{x}$.

3.1.3 Discrete case

In practice, the fields have to be represented with a finite spherical harmonics expansion. At ECMWF, a triangular truncation ($n \leq n_{max}$) is being used, but the above development would also be valid for the other truncation types (rhomboidal or trapezoidal). All the above computations are currently made in the Laplace space, the summations over n being limited to n_{max}.

For a field $\mathbf{z}$ decomposed in a finite spherical hamonics expansion, one has

$$\frac{1}{4\pi}\int_{\Sigma}\mathbf{z}^2 d\Sigma = \sum_{n=0}^{n_{max}}\sum_{m=-n}^{n}\mathbf{z}_n^m\mathbf{z}_n^{m*} = \sum_{n=0}^{n_{max}}\left\{\mathbf{z}_n^{0^2} + 2\sum_{m=1}^{n}\left(\mathbf{z}_{nr}^{m^2} + \mathbf{z}_{n_i}^{m^2}\right)\right\} \tag{27}$$

In the spectral models, a colocation grid is used for evaluating the nonlinear terms of the equations of evolution (Bourke, 1972). It is defined as a set of i_{max} colatitudes θ_i used for the Gaussian quadrature, with Gaussian weights ω_i in the North-South direction and a set of j_{max} longitudes λ_j used for the Fourier transform in the East-West direction. The Parseval formula has a discrete equivalent, provided the grid has enough resolution ($j_{max} \geq 1 + 2n_{max}$ and $i_{max} \geq 1 + n_{max}$)

$$\frac{1}{4\pi}\int_{\Sigma}\mathbf{z}^2 d\Sigma = \sum_{n=0}^{n_{max}}\left\{\mathbf{z}_n^{0^2} + 2\sum_{m=1}^{n}\left(\mathbf{z}_{nr}^{m^2} + \mathbf{z}_{n_i}^{m^2}\right)\right\} = \frac{1}{j_{max}}\sum_{i=1}^{i_{max}}\omega_i\sum_{j=1}^{j_{max}}\mathbf{z}(\lambda_j,\theta_i)^2 \tag{28}$$

Courtier and Naughton (1994) show that the Parseval formula remains valid to machine precision with an appropriately defined reduced Gaussian grid. Therefore it could have also been possible to evaluate the summation in grid point space which, as we shall see under subsection (vi), introduces further flexibility in the formulation.

3.1.4 Isotropic correlations.

As early as Rutherford (1972), it was noted that in operational meteorology the assumption of isotropic correlations was by far superior to isotropic covariances. It allows account to be taken of the contrast between data rich and data poor areas which leads to different quality in the subsequent short range forecast. Such a feature was implemented in the operational ECMWF OI (Shaw *et al.* 1987).

The random field ξ is, as above, assumed unbiased, but we now assume the correlation to be isotropic instead of the covariances. Let us denote the variances of ξ by σ_b^2. The normalized field $\xi' = \xi/\sigma_b$ is of isotropic covariances with variance equal to 1. It is therefore possible to apply the result of the previous paragraph and

$$J_b(\delta\mathbf{x}) = \sum_n\sum_{m=-n}^{n}\delta\mathbf{x}'^m_n\delta\mathbf{x}'^{m*}_n\frac{\sqrt{2n+1}}{f_n} \tag{29}$$

with

$$\delta\mathbf{x}' = \frac{\delta\mathbf{x}}{\sigma_b}$$

f is the representation of an isotropic tensor of variance equal to 1. Equation (14) relates the variance of an isotropic covariance tensor to the f_n, therefore

$$\sum_n f_n\sqrt{2n+1} = 1 \tag{30}$$

This feature is implemented in the ECMWF 3D-Var but not in the NCEP SSI which is relaxing the isotropy of the covariances in spectral space (see below subsection viii).

3.1.5 Compactly supported correlations.

In most statistical models used so far in OI, the horizontal correlations essentially vanish beyond a distance of typically 2000 km in the troposphere (see e.g. HLLH86). HLLH86 used a decomposition in Bessel function series with a radius of the underlying cylinder of 3000 km while Bartello and Mitchell (1992) used a 3800 km radius. This may also be a desirable feature of the statistical model used in 3D-Var. Gaspari and Cohn (1997) developed the theory for the construction of compactly supported correlations in two and three dimensions that we follow in the remainder of this section. The basic idea is to define a compactly supported function and through self-convolution to obtain a correlation function which, by construction is compactly supported.

Given a covariance tensor $\mathbf{T}$ represented by the function f, we have seen with Eq. (24) how to generate the function $f^{\frac{1}{2}}$ which represents the covariance tensor $\mathbf{T}^{\frac{1}{2}}$. Define the function $\tilde{f}^{\frac{1}{2}}$, resetting the function $f^{\frac{1}{2}}$ to 0 beyond a given distance. $\tilde{f} = \tilde{f}^{\frac{1}{2}} * \tilde{f}^{\frac{1}{2}}$ is a correlation function since its Legendre coefficients expansion are positive by construction, as seen from Eq. (16). Furthermore $\tilde{f}$ is compactly supported. However the Legendre expansion cannot be finite (Gaspari and Cohn, 1997), nevertheless we found in practice that finite expansion were obtained with $\tilde{f}$ compactly supported within machine precision. This is further discussed in Part II of this paper.

This feature is implemented neither at ECMWF nor at NCEP, and we shall see in Part II that it is most likely a weakness of the current implementation. It has later been implemented in the 1997 revision of 3D-Var at ECMWF.

3.1.6 Horizontally variable length scale.

Generally, the operational implementation of OI used different length scales, depending on the geographic location thus allowing for a broader length scale in data poor areas than in data rich areas. This was empirically found useful in operational practice and justified using a 2-dimensional Kalman filter by Bouttier (1994).

Consider two isotropic covariance tensors $\mathbf{T}_1$ and $\mathbf{T}_2$ and two complementary subdomains Σ_1 and Σ_2 of the sphere Σ. Define $\mathbf{z}_1 = \mathbf{T}_1^{-\frac{1}{2}}(\bullet, \delta\mathbf{x})$ and $\mathbf{z}_2 = \mathbf{T}_2^{-\frac{1}{2}}(\bullet, \delta\mathbf{x})$. J_b may now be defined as

$$J_b = \frac{1}{4\pi} \int_{\Sigma_1} \mathbf{z}_1^2 d\Sigma + \frac{1}{4\pi} \int_{\Sigma_2} \mathbf{z}_2{}^2 d\Sigma \tag{31}$$

In the discrete case, the two integrals may be evaluated in grid point space, making use of the Parseval formula. This could easily be generalized to a few subdomains, the limitation being the cost induced since a set of spectral transform is required per subdomain. Neither the ECMWF 3D-Var nor the NCEP SSI have incorporated this feature so far. Nevertheless we shall see in Part III that it would be desirable, the typical length-scale of the short range forecast errors being shorter over data dense areas like the Northern Hemisphere continents than over data poor areas like the oceans (Bouttier, 1994).

3.1.7 Relationship with Bessel function expansions.

As OI was implemented solving Eq. (6) locally, the statistical model only needed to be defined on the tangent plane to the sphere. Then, following Gandin (1963) and Rutherford (1972), HLLH86 and Bartello and Mitchell (1992) used Bessel function expansions to represent the correlation functions of the OI statistical model. In order to be able to relate the 3D-Var statistical model to those used with OI, it is therefore necessary to study its behaviour in the limit of small angular separation, when the tangent plane approximation makes sense, i.e. when the horizontal distance is small compared to the radius of the sphere.

¿From formula (9.1.71, p362) of Abramowitz and Stegun (1965) or formula A.2.2 of Courtier and Naughton (1994), we find that for large n and small θ such that the product $n\theta$ remains fixed,

$$P_n^0(\cos\theta) \approx \sqrt{2n+1}\mathcal{J}_0(n\theta) \tag{32}$$

Equation (11) then becomes

$$f(\theta) \approx \sum_n f_n\sqrt{2n+1}\mathcal{J}_0(n\theta) \tag{33}$$

HLLH86 require the derivative of the correlation to be 0 at some distance d (3000 km in their case, 3800 km in Bartello and Mitchell, 1992). This allows Eq. (33) to be rewritten as

$$f(\theta) \approx \sum_n f_n\sqrt{2n+1}\mathcal{J}_0\left(\frac{nd}{a}\frac{a\theta}{d}\right) \tag{34}$$

and therefore to interpret $k_n = nd/a$ as the wavenumber in the Bessel function expansion since $-(k_n/d)^2 = -(n/a)^2$ is the eigenvalue of the Laplacian operator in polar coordinates with $\mathcal{J}_0(n\theta)$ as eigenfunction. In Part II the power spectrum specified in 3D-Var will be compared with the results of previous studies, using Eq. (34).

HLLH86 relates k_n to an equivalent total wavenumber n using $(k_n/d)^2 = n(n+1)/a^2$. In practice the difference is half of a wavenumber, except for wavenumber 0 where there is no difference and where the interpretation does not make a lot of sense.

3.1.8 Relaxing the isotropy.

In Eq. (20) which defines J_b in spectral space for an isotropic covariance tensor, it is possible to introduce a dependance of the b coefficients not only with total wave number n, but with both total wavenumber n and zonal wavenumber m thus still keeping the spherical harmonics orthogonal for the metric defined by the covariance tensor. This is a feature operationally implemented in the NCEP SSI.

Let us assume that the tensor $\mathbf{T}$ is invariant to rotation about the polar axis. As a consequence, the different zonal wavenumbers m are decoupled from each other, and in spectral space, the matrix of $\mathbf{T}$ is block diagonal, with a block for each wavenumber m. If in addition, $\mathbf{T}$ is symmetric with respect to a meridian plane, the imaginary and real part of a given wavenumber m are decoupled, each block being equal. Furthemore, the symmetry with respect to the equator decouples the odd from the even harmonics (the parity of an harmonic is defined as the parity of $n - m$, an even harmonic is symmetric with respect to the equator while an odd one is antisymmetric).

In the tangent plane to the sphere at given colatitude θ, the covariance tensor may be approximated to second order in both coordinate directions. The iso-covariances are then ellipses. The above symmetry properties require the two axes of the ellipse to be parallel to the axes of coordinates. In addition, at the Northern pole, the ellipse reduces to a circle.

The orthogonality of the spherical harmonics for the metric defined by the covariance tensor implies some further properties that have not been investigated. For example the variances may also have a latitudinal variability since the spherical harmonics expansion of the Dirac distribution at the Northern pole depends only on the zonal harmonics while the Dirac distribution at the equator depends on all zonal wavenumbers.

3.2 Univariate case, tridimensional.

Just as the ECMWF model, 3D-Var exploits the shallowness of the atmosphere by assuming the metric defined over the space of atmospheric fields to be independent of the vertical (Müller, 1989). The equipotentials are assumed spherical and therefore at the same distance a from the centre of the Earth (Phillips, 1973). A vertical coordinate is then chosen which, say, varies from 0 at the top of the atmosphere to 1 at the bottom. This vertical coordinate may be the σ-coordinate as at NCEP or the hybrid η-coordinate of Simmons and Burridge (1981).

It is important to realize at this stage that the notion of horizontal isotropy is not intrinsic and depends on the choice of vertical coordinate. This is a consequence of the degeneracy of the metric in the vertical direction which implies that for any vertical coordinate, the coordinate surfaces are horizontal, i.e. orthogonal to the normal direction to the equipotentials. If there is no ambiguity, we shall use in the following "horizontal isotropy" with respect to the η-surfaces.

A three-dimensional atmospheric field x may be expanded in terms of the spherical harmonics to obtain

$$\mathbf{x} = \sum_n \sum_{m=-n}^{n} \mathbf{x}_n^m(\eta) Y_n^m \tag{35}$$

The covariance tensor $\mathbf{T}$ is assumed invariant to rotation. Fixing the value of the vertical coordinate η in the first entry of $\mathbf{T}$ and η' in the second entry, one obtains a covariance tensor defined over the sphere and, being the trace of an isotropic covariance tensor, is itself isotropic. Therefore one may apply the bidimensional result of Eq. (9)

$$\mathbf{T}(Y_n^m \delta_\eta, Y_{n'}^{m'*} \delta_{\eta'}) = \delta_{n-n'} \delta_{m-m'} b_n(\eta, \eta') \tag{36}$$

$b_n(\eta, \eta')$ can be interpreted as the covariance between level η and level η' for the horizontal scale associated to the total wavenumber n. In the vertically discretized case, the isotropic covariance tensor has a block diagonal expression. A vertical covariance matrix $\mathbf{B}_n$ consisting of the $b_n(\eta,\eta')$ may be defined for every total wave number n. All the bidimensional results of the previous section may then be generalized to the three-dimensional case. As an illustration, the vertical covariance matrix, denoted by $\mathbf{B}$, is obtained from the matrices $\mathbf{B}_n$ with

$$\mathbf{B} = \sum_n \mathbf{B}_n(2n+1) \tag{37}$$

which is the equivalent of Eq. (14).

Remark 1. Such a statistical model is, in general, non separable in that the covariance between two points cannot be expressed as the product of a function of the horizontal distance with a function of the vertical separation. Separability implies that the matrices $\mathbf{B}_n$ are obtained as the product of a vertical covariance matrix, independent of n, with a spectrum, independent of the vertical. The ECMWF OI relied on this hypothesis, apart from a large scale term in the geopotential covariance which was uncorrelated with stream function or velocity-potential.

Remark 2. A hierarchy of non separable models may be introduced ranging between the general formulation and the separable formulation. If in the separable formulation, one introduces a spectrum which depends on the vertical, the length-scale could vary with the vertical. Another possibility would be to assume the EOF of the matrices $\mathbf{B}_n$ to be independent of n. None of those formulations were found to be in close agreement with the empirical statistics which is why we retained the general formulation.

Remark 3. As the ECMWF OI relied on a Bessel function expansion, it would have been straightforward (but of significant cost) to implement a nonseparable statistical model similar to that of 3D-Var.

Remark 4. The isotropic correlations are obtained, as in the bidimensional case, by first dividing in grid point space by the standard deviations of background errors. This procedure may be generalized by dividing in grid point space by the (spatially variable) square root of the vertical covariance matrix of background error. This introduces spatial variability of the vertical covariance matrix. This generalization is not in the first implementation of the ECMWF 3D-Var.

3.3 Winds

3.3.1 Bidimensional.

The wind field is uniquely decomposed over the sphere into divergent and rotational components obtained from the velocity potential χ and stream function ψ respectively. Isotropy is assumed for the covariance tensor of the doublet (χ, ψ) which implies a block-diagonal structure in spectral space with a 2-2 square matrix which depends on the the total wave number n only for every doublet $(\chi^m_{nr}, \psi^m_{nr})$ or $(\chi^m_{n_i}, \psi^m_{n_i})$. No correlation between the rotational and divergent component further translates in diagonal 2-2 matrices.

Isotropic correlations are considered as in the scalar case by dividing in grid point space by the standard deviations of background errors. However, it is not equivalent to perform this normalization for the wind field as compared to the stream function and velocity potential. In order to keep the velocity potential and the stream function independent, the normalization should not be performed on the wind field. In practice, this is critical since the divergence field is an order of magnitude smaller than the vorticity field.

3.3.2 Tridimensional.

The above results are generalized in practice to the tridimensional case following what was done for the scalar fields. Nevertheless there is a hidden difficulty which we detail now. The wind field is defined as the velocity of an air parcel along the equipotentials. However in 3D-Var, as in the ECMWF model, the horizontal derivatives are taken along the coordinate surfaces. Consequently the stream function, the velocity potential, as well as the vorticity and the divergence are concepts which depend on the choice of vertical coordinate. No practical problems have been found (yet!), however they are likely to arise at high resolution close to orography in relation to the multivariate formulation.

3.4 Multivariate formulation.

The multivariate formulation of 3D-Var is discussed in detail in Courtier *et al.* (1993) and we shall summarize in this section the main features. Parrish and Derber (1992) diagnose the balanced part of the mass field from the vorticity field using a variant of the balance equation accounting for some divergence effects. The control variable consists then of the vorticity, the divergence and the unbalanced part of the mass field. We have followed another route, remaining closer to nonlinear normal mode initialization, this is what is described below. The results of the experimentation presented in part III revealed several weaknesses, leading to a revised formulation described in Bouttier *et al.* (1997) and which is very close from Parrish and Derber (1992) for the multivariate aspects.

In the vicinity of a state of rest, the slow manifold is tangent to the Rossby linear manifold R (see e.g. Daley, 1991 for a thorough description of the concepts used here and Courtier *et al.* 1993 for the implications for 3D-Var). As 3D-Var is using a spectral representation of the fields, the Rossby linear manifold is readily accessible and the projection on R consists of linear normal mode initialization. $\delta\mathbf{x}$ is separated into three components, namely a Rossby component $\delta\mathbf{x}_r$, a gravity component $\delta\mathbf{x}_g$, and an univariate component $\delta\mathbf{x}_u$.

In midlatitudes, the univariate component is set to 0, while the gravity component is penalized to a degree which depends both on the total wavenumber n and the vertical scale (the index being the rank of the eigenvector of the vertical covariance matrix). This dependence on both horizontal and vertical scale has been found in the empirical statistics, and for example the dependence on the horizontal scale was implemented in the ECMWF OI following the results of HLLH86.

In the tropics, the gravity and Rossby components are set to 0, the analysis is then univariate, but the divergence field of the univariate component remains penalized. In the latitude band 15-30 a smooth transition from the midlatitude to the tropical analysis is implemented. This mimics the ECMWF OI.

The vertical staggering of the ECMWF model introduces a spurious $2\delta\eta$ noise in the vertical while going back from the mass variable $P = \phi + RTln(p_s)$ to temperature T and surface pressure p_s, ϕ being the geopotential. The noise reached an amplitude of a few degrees in the stratosphere. This was solved by the use of a pseudo inverse of the integration of the hydrostatics consistent with the vertical covariance matrices (see Courtier *et al.* 1993 for a comprehensive discussion).

In order to avoid double counting in the evaluation of J_b, only the contribution of vorticity accounts for the Rossby component, only the contribution of divergence and mass accounts for the gravity component while the three are considered for the univariate component. The first two total wavenumbers of the mass field are also considered in the evaluation of J_b of the Rossby component since they depend weakly, if at all, on vorticity.

The ECMWF implementation of OI required a special treatment of the tides (Wergen, 1988), similar difficulties have been encountered in the early experimentation of 3D-Var. The 12 hour periodicity of the radiosondes network, the two heliosynchronous NOAA satellites in quadrature, the six hour cycle of the assimilation, all are in potential resonnance with the natural frequencies of the atmospheric tides, and diurnal and semidiurnal oscillations of the assimilation increments were clearly visible out of an harmonic analysis performed over two weeks assimilations. In essence the modification introduced to the background term is an adequate penalization of the tidal contribution performed in spectral space, followed by nonlinear normal mode initialization of the increments (see section 5.1).

Surface pressure forecasts plotted every timestep at selected gridpoints showed that the above formulation was able to control fast surface pressure oscillations to a large extent with a maximum amplitude in the remaining oscillations of a fraction of a millibar. The introduction in the objective function of a term J_c measuring the distance to the slow manifold as in Courtier and Talagrand (1990) eliminated the remaining oscillations, even close to orography. This term comprises the square norm of the tendencies of the gravity waves.

4 Observations.

The observation operators provide the link between the analysis variables and the observations (Lorenc, 1986, Pailleux, 1990). The operator H in Eq. (3) signifies the ensemble of operators transforming the control variable $\mathbf{z}$ into the equivalent of each observed quantity, $\mathbf{y}^o$, at observation locations. The 3D-Var implementation allows H to be (weakly) non-linear, which is seen to be an advantage for the use of TOVS radiance data, for example.

In this section we outline the content of the observation operators and describe the observational data used in 3D-Var.

4.1 Observation operators

The operator H is subdivided into a sequence of operators, each one of which performs part of the transformation from control variable to observed quantity: i) The inverse change of variable converts from control variables to model variables. ii) The inverse spectral transforms put the model variables on the model's reduced Gaussian grid. iii) A 12-point bi-cubic horizontal interpolation gives vertical profiles of model variables at observation points. The surface fields are interpolated bi-linearly to avoid spurious maxima. The three steps i) to iii) are in common for all data types. Thereafter follows iv) vertical integration of for example the hydrostatic equation to form geopotential, and of the radiative transfer equation to form radiances (if applicable), and v) vertical interpolation to the level of the observations. The vertical operations depend on the variable. The vertical interpolation is linear in pressure for temperature and specific humidity, and it is! linear in the logarithm of pressure for wind. The vertical interpolation of geopotential is similar to wind (in order to preserve geostrophy) and is performed in terms of departures from the ICAO standard atmosphere for increased accuracy (Simmons and Chen, 1991, see Appendix A). The geopotential vertical interpolation together with the temperature vertical interpolation are not exactly consistent with hydrostatism, the emphasis having been put on accuracy. Nevertheless consistent and accurate vertical interpolation could be devised, which may be important for intensive use of temperature information.

The vertical interpolation operators for SYNOP 10m-wind and 2m-temperature match the model's surface layer parametrisation. The vertical gradients of the model variables vary strongly in the lowest part of the boundary layer, where flow changes are induced on very short time and space scales, due to physical factors such as turbulence and terrain characteristics. The vertical interpolation operator for those data takes this into account following Monin-Obukhov similarity theory. Results using such operators, which are inspired from Geleyn (1988) have been presented by Cardinali *et al.* (1994). It was found that T2m data could not be satisfactorily used in the absence of surface skin temperature as part of the control variable, as unrealistic analysis increments appeared in the near-surface temperature gradients. The Monin-Obukhov based observation operator for 10m wind on the other hand is used for SYNOP and DRIBU winds. Scatterometer 10-m winds, however, are used th! rough a simple logarithmic relationship between lowest model level wind (at approximately 32m) and wind at 10m. Relative humidity is assumed constant in the lowest model layer to evaluate its 2m value.

$$u_{10m} = u_{32m}\frac{ln(10/z_0)}{ln(32/z_0)}$$

where z_0 denotes the surface roughness length. H has been expressed as the product of individual operators. The variational analysis procedure requires the gradient of the objective function with respect to the control variable. This computation makes use of the adjoint of the individual tangent linear operators, applied in the reverse order. Operators also exist for SATEM precipitable water content and SSM/I total precipitable water data, but these data are currently not used operationally, nor in the experiments reported in Part III.

The details regarding observation operators for conventional data can be found in Vasiljević *et al.* (1992). The TOVS observation operator has been described by Andersson *et al.* (1994) and the use of scatterometer data by Gaffard *et al.* (1997).

4.2 Data usage

Observation operators for all observation types that were used by OI have also been implemented in 3D-Var. In addition 3D-Var uses TOVS cloud-cleared radiances and scatterometer ambiguous winds. Table 1 lists the observing systems currently used by 3D-Var in ECMWF's operational data assimilation. The table also indicates important restrictions on data usage and thinning of data. The TOVS data are further discussed in Part III. 3D-Var (like OI) uses the data from a six-hour time window centred at the analysis time. If there are multiple reports from the same fixed observing station within that time window, the data nearest the analysis time are selected for use in the analysis. Some thinning is applied for the moving platforms reporting frequently.

Table 1: Observations used by 3D-Var in ECMWF's operational analyses in 1996.

Obs. type	Observed variable	Remark
SYNOP	Surface pressure	Not used if more than 800 m below model orography
	10 m wind	from SHIP and some tropical island stations
	2m relative humidity	Not used if more than 50 m below model orography
AIREP	Wind	thinned to approximately 200 km along flight
	Temperature	thinned to approximately 200 km along flight
SATOB	Wind	Meteosat, GOES and GMS. Not over land in Northern Hemisphere nor over land for low-level winds
DRIBU	Surface pressure	
	10 m wind	
TEMP	Geopotential height	maximum 15 levels (priority to standard levels)
	Wind	maximum 15 levels (priority to standard levels)
	Specific humidity	below 300 hPa
PILOT	Wind	maximum 15 levels (priority to standard levels)
TOVS	Cloud cleared radiances	tropospheric channels over oceans only south of 70 N
	1D-Var retrieval	north of 70 N
SATEM	NESDIS retrieval	above 100 hPa poleward of 20.
PAOB	Surface pressure	south of 20 S
SCAT	Ambiguous winds	if both observed and model wind speeds are less than 20 ms^{-1}

4.3 Observation error covariances

Initially, the OI standard deviations of observation errors were used in 3D-Var. However the J_o diagnostics in 3D-Var (before minimization) showed that there was a mis-specification of the observation error standard deviation, σ_o, for several data types. Particularly SATOB and DRIBU winds had σ_o too large, and humidity errors were generally too small. Average J_o-ratios (defined as J_o/N_{obs} where N_{obs} is the number of observations) were computed from a 3D-Var assimilation, and compared with the statistical expectation of the J_o-ratio, which is $< J_o/N_{obs} >= (\sigma_o^2+\sigma_b^2)/\sigma_o^2$. We can see that even with a perfect background, the ratio should not be less than 1, and with $\sigma_b \approx \sigma_o$ it should be close to 2. This lead to modifications of the specified σ_o for a number of observation types. The observation errors currently used are tabulated in Appendix B. The observation errors for TOVS radiance data were taken from Eyre *et al.* (1993), and are also listed in Appendix B.

The observation error is assumed uncorrelated (i.e. the matrix $\mathbf{R}$ is diagonal) for all data except radiosonde geopotential data, TOVS radiance data and SATEM thicknesses. The radiosonde geopotential data are vertically correlated using a continuous covariance function $ae^{-b(x_1-x_2)^2}$ where a is 0.8, b a tuning constant close to 1 and x_1 and x_2 are transformation values, based on a sixth degree polynomial in $ln(p)$ of the two pressures involved. This is the same as previously used in ECMWF OI. The vertical correlation of SATEM thickness data is as described in Kelly and Pailleux (1988). The horizontal correlation of SATEM and TOVS observation errors are assumed Gaussian, both with a length scale of 350 km. Only half of the observation error is assumed to be correlated. The implementation has been described by Andersson *et al.* (1994), with in particular arbitrary groupings of 120 data. The inter-channel correlation of radiance observation error is assumed to be zero. The horizontal correlation of SATEM and TOVS observation errors is no longer accounted for in ECMWF operations since end of September 1996. The effect on analysis and forecast accuracy is small.

5 Practical implementation.

5.1 Incremental formulation.

As mentioned earlier in the description of 3D-Var, the formulation used is incremental (Courtier *et al.* (1994)). The cost is then comparable to the cost of OI. This implies that two different resolutions are used for the comparison with observations (T213L31) and minimisation (T63L31). Three different steps are performed: the comparison of the background with the observations at high resolution to compute the innovation vectors, the minimisation at low resolution to produce low resolution analysis increments, and finally the comparison of the analysis field with observations.

A truncation operator allows one to go from high resolution fields to low resolution. For the spectral upper-air fields, this is simply a truncation at wavenumber 63. The grid-point fields are first transformed to spectral space, then truncated, and transformed back to grid-point space. In that way, spectral upper-air fields and surface grid-point fields used in the minimisation are consistent.

The analysis field is the sum of the background and of the pseudo-inverse of the truncation operator applied to the low resolution increments. This pseudo-inverse consists in filling in the spectral wave-numbers greater than 63 by 0., and then applying adiabatic non-linear normal mode initialisation ($NNMI$) to the increments in order to adjust the high wave-numbers to the orography at high resolution. This is performed by evaluating

$$\mathbf{x}_a(HR) = \mathbf{x}_b(HR) + NNMI(\mathbf{x}_b(HR) + \delta\mathbf{x}_a(LR)) - NNMI(\mathbf{x}_b(HR))$$

where HR and LR stands for high and low resolution respectively. This is necessary since the analysis obtained at the end of the minimization procedure is balanced but for an orography truncated at wavenumber 63.

As far as the humidity is concerned, the control variable used in the minimisation is specific humidity in spectral space. There is no constraint forcing the minimisation to produce positive and non supersaturated values for this quantity. However, before the computation of observation departures in the minimisation stage, grid-point values are replaced by $f(q, qsat)$ where f is a differentiable function such that it results in positive and not super-saturated humidity values. The high resolution analysis is modified by resetting negative humidities to zero and supersaturated values to saturated values.

5.2 Preconditioning

As already explained in section 3.(a).(ii), one generally uses the Hessian of the background term J_b to precondition the problem. One implementation is to use the change of variable $\mathbf{z} = \mathbf{B}^{-1/2}\delta\mathbf{x}$. In practice, this was not found to be practical in the current formulation of 3D-Var where the J_b computation involves splitting the increment $\delta\mathbf{x}$ into three parts: the Rossby part, the gravity-wave part and a univariate part.

5.3 Minimisation.

The minimisation problem involved in this 3D-Var can be considered as large-scale, since the number of degrees of freedom in the control variable is slightly over 500000. An efficient descent algorithm was provided by the Institut de Recherche en Informatique et Automatique (INRIA, France). It is a variable- storage quasi-Newton algorithm described in Gilbert and Lemarechal (1989). The method uses the available in-core memory to update an approximation of the Hessian of the cost function. In practice, ten updates of this Hessian matrix are used. The approximation is modified during the minimisation by deleting information from the oldest gradient and inserting information from the most recent one. The number of iterations is limited to 70. Only very small adjustments of the analysis occur during the second half of the minimisation. On the whole, the cost function is typically divided by a factor of 2 and the norm of the gradient by a factor of 20. The approximation of the Hessian computed during a given analysis 24 hour ago is used as a first estimate for the corresponding analysis today.

6 Numerical illustrations

Single-observation analysis are used to exhibit the structure functions as actually specified in variational assimilation since the analysis increments are then proportional to the covariances of the background errors in model space with the background errors in the observation space for the observation considered. This is explained in detail in Thépaut *et al.* (1996) who applied this approach to compare the statistical models of 3D-Var and 4D-Var for the height field in the case of a mid-latitude cyclogenesis. We follow the same approach to illustrate the multivariate aspects of 3D-Var.

Figures 1 and 2 show the results of such single observation experiments with the background error statistics as obtained in Part II. The observations are located at 60 N and at the Equator respectively. Horizontally constant standard deviations of background errors have been specified and J_c was not used. The three rows are for observation of 500 hPa geopotential height (top), u-component (middle) and v-component (botom) of the 500 hPa wind. The three columns show the response in terms of height, u and v, respectively. The results have been expressed in terms of correlations, computed from the analysis increments by normalization with the effective standard deviations of background errors (following Thépaut *et al.* (1996) in their 3D-Var results). As expected, the results in mid-latitudes (Fig. 1) are near-geostrophic, and they are in close agreement with those shown in similar diagrams in Daley (1991), Mitchell *et al.* (1990) and Bartello and Mitchell (1992), for example. The unusual shape of the negative lobes of the u-u correlations was also found by Bartello and Mitchell. Our results indicate that the u-z and z-u correlations have slightly higher magnitude to the south than to the north of the observation. This is due to the variation in the coriolis parameter f. The results on the Equator (Fig. 2) show that the mass/wind coupling is very weak as expected from the univariate tropical formulation, with the wind increments mostly non divergent.

The two cross-sections in Fig. 3 show the u-u (a) and u-T (b) covariances in a north-south vertical plane. It can be seen that in a vertical column the u-u covariances diminish more rapidly downward than upward which confirms the result of Bartello and Mitchell 1992. This is an expression of the non-separability between the horizontal and vertical directions of the background error structure functions, as will be dicussed further in Part II. As a consequence u-T covariances (Fig. 3b) tend to slope upwards, away from the observation.

7 Conclusion.

The general conclusion of this three-part paper is deferred to the last part and we only discuss the specifics of the formulation. We have shown in this paper that it is possible to account within 3D-Var for most features of optimal interpolation. With respect to the ECMWF OI, the 3D-Var statistical model has been refined to incorporate non-separability in a way similar to that suggested by Phillips (1986). The multivariate formulation makes use of the Hough functions which paves the way toward a formulation which would produce analysis increments tangent to the slow manifold. Nevertheless, the present multivariate formulation does not have an explicit square root. This is a weakeness for the preconditioning, which assumes for example that the vertical correlations of divergence and vorticity are kept the same for a given total wavenumber. In addition, the simplified Kalman filter as proposed by Courtier (1993) requires a square-root formulation. In the present formulation, J_b is evaluated in spectral space; it would be possible to evaluate it in Hough modes space, since recent ECMWF developments toward a simplified Kalman filter imply smoother background error standard deviations than those of OI.

No progress has been made in the formulation of 3D-Var in the tropics as compared to OI. The horizontally variable vertical structure functions, when implemented, may allow reconsideration of the balance aspects. 3D-Var analyses simultaneously the mass, wind and humidity fields. However the humidity field remains largely decoupled from the others in the present formulation. A significant step forward may be expected from a proper coupling of the mass and wind fields with the humidity field.

Significant difficulties have been encountered in practice with the treatment of the tidal waves. With the 6-hour cycling used in 3D-Var, any misspecification of the semidiurnal tidal wave can be interpreted as a $2\Delta t = 12 hours$ oscillation of the analysis increments. The difficulty is three-fold : such an oscillation is a non dissipated solution of the model equations; any biases in the model or the conventional network will alias the tides; any biases in the two

TOVS satellites, one with respect to the other, will alias the semidiurnal tide as they are in quadrature. The initialization of the large-scale component of the analysis increments cured the problem to a large extent. Nevertheless this remains a challenge for a future improvment of the data assimilation system.

Two potential weaknesses of 3D-Var related to the vertical coordinate have been exhibited. The performance of 3D-Var will have to be carfully monitored in the vicinity of orography, and specific remedies may have to be devised.

The incremental formulation may be extended to the vertical following Gauthier *et al.* (1996) who devised a 3D-Var formulation in pressure coordinates. In particular this may be a significant improvement if the isotropy hypothesis is better satisfied in the free atmosphere along e.g. potential temperature surfaces. For the horizontal aspects, a computational sphere may be introduced with the isotropy being applied over this sphere. The mapping between the geographical sphere and the computational sphere could rely on the semi-geostrophic coordinates as proposed by Desroziers and Lafore (1993) over the plane.

Acknowledgements

The first author would like to thank P.Gauthier for very fruitful discussions in Montréal during July 1996. The development of 3D-Var greatly benefited from the Arpege-IFS collaboration, particularly from the contribution of Jean-Noël Thépaut, Patrick Moll, Philippe Caille, Per Undén and the ECMWF data division.

Fréderic Delsol and Dave Burridge believed in the variational project in 1986-1987, Michel Jarraud, Jean-François Geleyn and Michel Rochas, on the continent, realized that this dream (or probably nightmare for some!) may be transformed in a palpable project.

The "Groupement de Recherche sur les Méthodes variationnelles en Météorologie et Océanographie" funded by the "Centre National de la Recherche Scientifique" and Météo-France has financially supported the variational project from 1988 to 1996, with the Director, Olivier Talagrand being a staunch supporter, particularly as the Chairman of the ECMWF Scientific Advisory Committee.

Adrian Simmons and Peter Houtekamer are aknowledged for their valuable comments on a first version of the manuscript. John Derber highlighted several weaknesses of this formulation.

A. The observation operator for geopotential height.

The geopotential at a given pressure p is computed by integrating the hydrostatic equation analytically using the ICAO temperature profile and vertically interpolating $\Delta\phi$, the difference between the model level geopotential and the ICAO geopotential. The ICAO temperature profile is defined as

$$T_{ICAO} = T_0 - \frac{\Lambda}{g}\phi_{ICAO} \tag{38}$$

where T_0 is 288K, ϕ_{ICAO} is the geopotential above 1013.25 hPa and Λ is 0.0065 K/m in the ICAO troposphere and 0 in the ICAO stratosphere. The ICAO tropopause is defined by the level where the ICAO temperature has reached 216.5 K. Using this temperature profile and integrating the hydrostatic equation provides T_{ICAO} and the geopotential ϕ_{ICAO} as a function of pressure. We may then evaluate the geopotential $\phi(p)$ at any pressure p following

$$\phi(p) - \phi_s = \phi_{ICAO}(p) - \phi_{ICAO}(p_s) + \Delta\phi \tag{39}$$

where p_s is the model surface pressure and ϕ_s the model orography. $\Delta\phi$ is obtained by vertical interpolation from the full model level values $\Delta\phi_k$. The interpolation is linear in $ln(p)$ up to the second model level and quadratic in $ln(p)$ for levels above it. The full model level values are obtained integrating the discretized hydrostatic equation following Simmons and Burridge (1981)

$$\Delta\phi_k = \sum_{j=Nlev}^{k+1} R_d(T_{v_j} - T_{ICAO_j})ln(\frac{p_{j+1/2}}{p_{j-1/2}}) + \alpha_k R_d(T_{v_k} - T_{ICAO_k}) \tag{40}$$

with

$$\alpha_k = 1 - \frac{p_{k-1/2}}{p_{k+1/2} - p_{k-1/2}} ln(\frac{p_{k+1/2}}{p_{k-1/2}})$$

for $k > 1$ and $\alpha_1 = ln(2)$.

B. Observation errors.

The observation error standard deviations currently assumed in the ECMWF 3D-Var are given in the tables below, for upper-air data and SYNOP heights (Table 2), surface data (Table 3), TOVS radiance data (Table 4) and SATEM retrieved thicknesses (Table 5). They include the instrumental error and the representativness error, and thus for the TOVS data, they include the forward model error. The TOVS observation errors in partly cloudy spots are inflated to 0.5, 0.9, 1.3, 0.9, 0.6 and 0.40 for channels HIRS-6, 7, 10, 13, 14 and 15, to account for any residual cloud contamination. Furthermore, the radiance observation errors are multiplied by a factor 1.5 when used in 3D-Var, because the data are sensitive to quantites such as temperature above the model top and surface temperature, which are currently not part of the 3D-Var control variable.

The relative humidity errors are specified according to a regression relation $\sigma_o = -0.0015T + 0.54$, for $240K < T < 320K$, obtained from a statistical analysis of their dependence with respect to temperature. Outside this interval, σ_o takes the values 0.18 and 0.06 rspectively. The standard deviations of error for the specific humidity is then deduced according to the tangent-linear relationship which relates specific and relative humidity, the linearization being performed in the vicinity of the observed values of temperature and humidity.

Table 2: Observations errors, upper air.

Pressure hPa	TEMP u/v ms^{-1}	SATOB u/v ms^{-1}	AIREP u/v ms^{-1}	PILOT u/v ms^{-1}	AIREP T K	TEMP Z m	SYNOP Z m
1000	2.3	2.0	2.5	2.3	1.4	4.3	7.0
850	2.3	2.0	2.5	2.3	1.4	4.4	8.0
700	2.5	2.0	3.0	2.5	1.2	5.2	8.6
500	3.0	3.5	3.5	3.0	1.2	8.4	12.1
400	3.5	4.3	4.0	3.5	1.2	9.8	14.9
300	3.7	5.0	4.0	3.7	1.3	10.7	
250	3.5	5.0	4.0	3.5	1.3	11.8	
200	3.5	5.0	4.0	3.5	1.4	13.2	
150	3.4	5.0	4.0	3.4	1.4	15.2	
100	3.3	5.0	4.0	3.3	1.4	18.1	
70	3.2	5.0	4.0	3.2	1.5	19.5	
50	3.2	5.0	4.0	3.2	1.6	22.5	
30	3.3	5.0	4.0	3.3	1.8	25.0	
20	3.6	5.0	4.0	3.6	2.0	32.0	
10	4.5	5.7	4.0	4.5	2.2	40.0	

Table 3: Observations errors, surface.

PAOB Z m	DRIBU Z m	SHIP Z m	SYNOP u/v ms^{-1}	DRIBU u/v ms^{-1}	SYNOP T K	SHIP T K	DRIBU T K
24.0	11.5	14.0	3.0	2.4	2.0	1.8	1.8

Table 4: Observations errors, TOVS radiances (K).

Channel		Error	Channel		Error	Channel		Error
HIRS	1	0.7	HIRS	10	0.8	MSU	2	0.3
	2	0.35		11	1.1		3	0.22
	3	0.3		12	1.5		4	0.25
	4	0.2		13	0.5			
	5	0.3		14	0.35			
	6	0.4		15	0.3			
	7	0.6						

Table 5: Observations errors, SATEM thicknesses (m).

	NESDIS		1D-Var		
	clear	p.cloudy cloudy	clear	p.cloudy	cloudy
1000-700	27.0	33.0	8.81	9.53	12.77
700-500	17.0	20.0	7.70	8.39	11.70
500-300	25.0	31.0	13.23	13.61	18.31
300-100	53.0	56.0	19.62	20.22	22.86
100-70	33.0	33.0			
70-50	36.0	36.0			
50-10	74.0	74.0			

References

Abramowitz, M. and Stegun, I. 1965 *Handbook of mathematical functions.*, Dover publications, Inc., New York

Andersson, E., Hollingsworth, A., Kelly, G., Lönnberg, P., Pailleux, J. and Zhang, Z. 1991 Global observing system experiments on operational statistical retrievals of satellite sounding data. *Mon. Wea. Rev.*, **119,** 1851–1864

Andersson, E., Pailleux, J., Thépaut, J.-N., Eyre, J. R., McNally, A. P., Kelly, G. A. and Courtier, P. 1994 Use of cloud-cleared radiances in three/four-dimensional variational data assimilation. *Q. J. R. Meteorol. Soc.*, **120**, 627–653

Andersson, E., Haseler, J., Undén, P., Courtier, P., Kelly, G., Vasiljević, D., Branković, C., Cardinali, C., Gaffard, C., Hollingsworth, A., Jakob, C., Janssen, P., Klinker, E., Lanzinger, A., Miller, M., Rabier, F., Simmons, A., Strauss, B., Thépaut, J.-N. and Viterbo, P. 1998 The ECMWF implementation of three dimensional variational assimilation (3D-Var). Part III: Experimental results. ECMWF Tech Memo 243. Submitted to *Q. J. R. Meteorol. Soc.*

Bartello, P. and Mitchell, H. L. 1992 A continuous three-dimensional model of short-range forecast error covariance. *Tellus*, **44A**, 217–235

Boer, G. J. 1983 Homogeneous and isotropic turbulence on the sphere. *J. Atmos. Sci.*, **40**, 154–163

Bourke, W. 1972 An efficient one level primitive equation spectral model. *Mon. Wea. Rev.*, **100,** 683–689

Bouttier, F. 1994 A dynamical estimation of forecast error covariances in an assimilation system. *Mon. Wea. Rev.*, **122**, 2376–2390

Bouttier, F., Derber, J., and Fisher, M. 1997 The 1997 revision of the J_b term in 3D / 4D-Var. ECMWF Tech. Memo. 238 (available from ECMWF)

Cardinali, C., Andersson, E., Viterbo, P., Thépaut, J.-N. and Vasiljević, D. 1994 Use of conventional surface observations in three-dimensional variational data assimilation. ECMWF Tech. Memo. 205 (available from ECMWF)

Cohn, S. E., Da Silva, A., Guo, J., Sienkiewicz, M., and Lamich, D. 1997 Assessing the effects of data selection with the DAO Physical-space Statistical Analysis System. *Mon. Wea. Rev.*, submitted.

Courtier, P. 1987 Application du contrôle optimal à la prévision numérique en météorologie. *Thèse de Doctorat de l'Université Pierre et Marie Curie*, Paris, France

Courtier, P. 1993 Introduction to numerical weather prediction data assimilation methods. *ECMWF seminar on developments in the use of satellite data in numerical weather prediction.*, 6–10 September 1993. pp 189–208.

Courtier, P. 1997 Dual formulation of four dimensional variational assimilation. *Q. J. R. Meteorol. Soc.*, **123**, to appear in the Oct. B issue

Courtier, P., Andersson, E., Heckley, W., Kelly, G., Pailleux, J., Rabier, F., Thépaut, J.-N., Undén, P., Vasiljević, D., Cardinali, C., Eyre, J., Hamrud, M., Haseler, J., Hollingsworth, A., McNally, A. and Stoffelen, A. 1993 Variational assimilation at ECMWF. ECMWF Tech. Memo. 194 (available from ECMWF)

Courtier, P. and Naughton, M. 1994 A pole problem in the reduced Gaussian grid. *Q. J. R. Meteorol. Soc.*, **120**, 1389–1407

Courtier, P. and Talagrand, O. 1987 Variational assimilation of meteorological observations with the adjoint vorticity equation. Part II. Numerical results. *Q. J. R. Meteorol. Soc.*, **113**, 1329–1347

Courtier, P. and Talagrand, O. 1990 Variational assimilation of meteorological observations with the direct and adjoint shallow-water equations. *Tellus*, **42A**, 531–549

Courtier, P., Thépaut, J.-N. and Hollingsworth, A. 1994 A strategy for operational implementation of 4D-Var, using an incremental approach. *Q. J. R. Meteorol. Soc.*, **120**, 1367–1388

Daley, R. 1991 *Atmospheric data analysis.*, Cambridge atmospheric and space sciences series, Cambridge University Press

Dee, D. P. 1995 On-line estimation of error covariance parameters for atmospheric data assimilation. *Mon. Wea. Rev.*, **123**, 1128–1145

Derber, J., Parrish, D. F. and Loord, S. J. 1991 The new global operational analysis system at the National Meteorological Centre. *Weather and Forecasting.*, **6**, 538–547

Desroziers, G. and Lafore, J.-P. 1993 Coordinate transformation for objective frontal analysis. *Mon. Wea. Rev.*, **121**, 1531–1553

Eyre, J. R. 1989 Inversion of cloudy satellite sounding radiances by nonlinear optimal estimation. *Q. J. R. Meteorol. Soc.*, **115**, 1001–1037

Eyre, J. R., Kelly, G. A., McNally, A. P., Andersson, E. and Persson, A. 1993 Assimilation of TOVS radiance information through one-dimensional variational analysis. *Q. J. R. Meteorol. Soc.*, **119**, 1427–1463

Eyre, J. R. and Lorenc, A. C. 1989 Direct use of satellite sounding radiances in numerical weather prediction. *Meteorol. Mag.*, **118**, 13–16

Flobert, J-F., Andersson, E., Chédin, A., Hollingsworth, A., Kelly, G., Pailleux, J. and Scott, N. A. 1991 Global data assimilation and forecast experiments using the Improved Initialization Inversion method for satellite soundings. *Mon. Wea. Rev.*, **119**, 1881–1914

Gaffard, C., Roquet, H., Hansen, B., Andersson, E. and Anderson, D. 1997 Impact of ERS-1 scatterometer wind data on the ECMWF 3D-Var assimilation system. To appear in *Q. J. R. Meteorol. Soc.*

Gandin, L. S. 1963 *Objective Analysis of Meteorological Fields.*, Leningrad, Gidromet.; Jerusalem, Israel Program for Scientific Translations, 1965.

Gaspari, G. and Cohn, S. 1997 Construction of Correlation Functions in two and three Dimensions. Submitted to *Q. J. R. Meteorol. Soc.*

Gauthier, P., Fillion, L., Koclas, P. and Charette, C. 1996 Implementation of a 3D variational analysis at the Canadian Meteorological Centre. *XI^th AMS Conference on Numerical Weather Prediction.* Norfolk, Virginia, 19^th–23^rd August 1996.

Geleyn, J. F. 1988 Interpolation of wind, temperature and humidity values from the model levels to the height of meaurement. *Tellus*, **40**, 347–351

Gel'Fand, I. M. and Vilenkin, N. Ya. 1964 *Generalized Functions, Vol. 4: Applications of Harmonic Analysis.*, Academic Press, New York and London.

Gilbert, J. C. and Lemaréchal, C. 1989 Some numerical experiments with variable storage quasi-Newton algorithms. *Math. Prog.*, **B25**, 407–435

Heckley, W., Courtier, P., Pailleux, J. and Andersson, E. 1992 The ECMWF variational analysis: general formulation and use of background information. *ECMWF workshop on variational assimilation with special emphasis on three-dimensional aspects*, 9–12 November 1992. pp 49–94

Hollingsworth, A. 1987 Objective analysis for numerical weather prediction., *Special volume J.Met.Soc.Jap.* "Short and Medium Range Numerical Weather Prediction", Matsuno T. ed., pp 11–60

Hollingsworth, A. and Lönnberg, P. 1986 The statistical structure of short-range forecast errors as determined from radiosonde data. Part I: The wind field. *Tellus*, **38A**, 111–136

Ide, K., Courtier, P., Ghil, M. and Lorenc, A. C. 1997 Unified notation for data assimilation: operational, sequential and variational. *J. Met. Soc. Japan*,**75**, 181–189

Kelly, G. and Pailleux, J. 1988 Use of satellite vertical sounder data in the ECMWF analysis system. ECMWF Tech. Memo. 143 (available from ECMWF)

Kelly, G., Andersson, E., Hollingsworth, A., Lönnberg, P., Pailleux, J. and Zhang, Z. 1991 Quality control of operational physical retrievals of satellite sounding data. *Mon. Wea. Rev.*, **119,** 1866–1880

Lönnberg, P. and Hollingsworth, A. 1986 The statistical structure of short-range forecast errors as determined from radiosonde data. Part II: The covariance of height and wind errors. *Tellus*, **38A**, 137–161

Lorenc, A. C. 1981 A global three-dimensional multivariate statistical interpolation scheme. *Mon. Wea. Rev.*, **109,** 701–721

Lorenc, A. C. 1986 Analysis methods for numerical weather prediction. *Q. J. R. Meteorol. Soc.*, **112,** 1177–1194

Lorenc, A. C. 1988 Optimal nonlinear objective analysis. *Q. J. R. Meteorol. Soc.*, **114,** 205–240

Lorenc, A. C. 1992 Iterative analysis using covariance functions and filters. *Q. J. R. Meteorol. Soc.*, **118,** 569–591

Lorenc, A. C. 1995 Development of an operational variational assimilation scheme. *WMO Int. Symp. on Assimilation of Observations in Meteorology and Oceanography.* Tokyo, Japan. 415–420

Mitchell, H.-L., Charette, C., Chouinard, C. and Brasnett, B. 1990 Revised interpolation statistics for the Canadian data assimilation procedure: Their derivation and application. *Mon. Wea. Rev.*, **118,** 1591–1614

Müller, R. 1989 A note on the relation between the "traditional approximation" and the metric of the primitive equations. *Tellus*, **41A,** 175–178

Pailleux, J. 1990 A global variational assimilation scheme and its application for using TOVS radiances. *WMO Int. Symp. on Assimilation of Observations in Meteorology and Oceanography.* Clermont-Ferrand, France. 325–328

Parrish, D. F. and Derber, J. C. 1992 The National Meteorological Center's spectral statistical interpolation analysis system. *Mon. Wea. Rev.*, **120,** 1747–1763

Parrish, D. F., Derber, J. C., Purser, J., Wu, W. and Pu, Z. 1995 The NMC global analysis system: Recent developments and future plans. *WMO Int. Symp. on Assimilation of Observations in Meteorology and Oceanography.* Tokyo, Japan. 403–407

Phillips, N. A. 1973 Principles of large scale numerical weather prediction. In *Dynamic meteorology.*, Ed. P.Morel, D. Reidel Publ. Comp., 1–96

Rabier, F., McNally, A., Andersson, E., Courtier, P., Undén, P., Eyre, J., Hollingsworth, A. and Bouttier, F. 1998 The ECMWF implementation of three dimensional variational assimilation (3D-Var). Part II: Structure functions. ECMWF Tech Memo 242. Submitted to *Q. J. R. Meteorol. Soc.*

Rutherford, I. 1972 Data ssimilation by statistical interpolation of forecast error fields. *J. Atmos. Sci.*, **29,** 809–815

Shaw, D.B., Lönnberg, P., Hollingsworth, A. and Undén, P. 1987 The 1984/1985 revisions of the ECMWF assimilation system. *Q. J. R. Meteorol. Soc.*, **113,** 533–566

Simmons, A. J. and Burridge, D. 1981 An energy and angular momentum conserving vertical finite difference scheme and hybrid coordinate. *Mon. Wea. Rev.*, **109,** 758–766

Simmons, A. J. and Chen, J. 1991 The calculation of geopotential and the pressure gradient in the ECMWF atmospheric model: Influence on the simulation of the polar atmosphere and on temperature analyses. *Q. J. R. Meteorol. Soc.*, **117**, 29–58

Talagrand, O. and Courtier, P. 1987 Variational assimilation of meteorological observations with the adjoint vorticity equation. Part I. Theory. *Q. J. R. Meteorol. Soc.*, **113,** 1321–1328

Thépaut, J.-N., Courtier, P., Belaud, G. and Lemaître, G. 1996 Dynamical structure functions in four-dimensional variational assimilation: A case study. *Q. J. R. Meteorol. Soc.*, **122,** 535–562

Thépaut, J.-N. and Moll, P. 1990 Variational inversion of simulated TOVS radiances using the adjoint technique. *Q. J. R. Meteorol. Soc.*, **116,** 1425–1448

Undén, P. 1989 Tropical data assimilation and analysis of divergence. *Mon. Wea. Rev.*, **117,** 2495–2517

Vasiljević, D., Cardinali, C. and Undén, P. 1992 ECMWF 3D-Variational assimilation of conventional observations. Proceedings of the ECMWF workshop on "Variational assimilation with emphasis on three-dimensional aspects.", Shinfield Park, Reading, RG2 9AX, 9–12 November 1992

Wergen, W. 1988 Diabatic Non-linear Normal Mode Initialisation for a spectral model. *Beitr. Phys. Atmosph.*, **61,** 274–302

Wunsch, C. and Stammer, D. 1995 The global frequency-wavenumber spectrum of oceanic variability estimated from TOPEX/POSEIDON altimetric measurements. *J. Geophys. Res.*, **100,** 24895–24910

Yaglom, A. M. 1987 *Correlation Theory of Stationary and related random functions, Vol. I: Basic results.*, Springer-Verlag, New York.

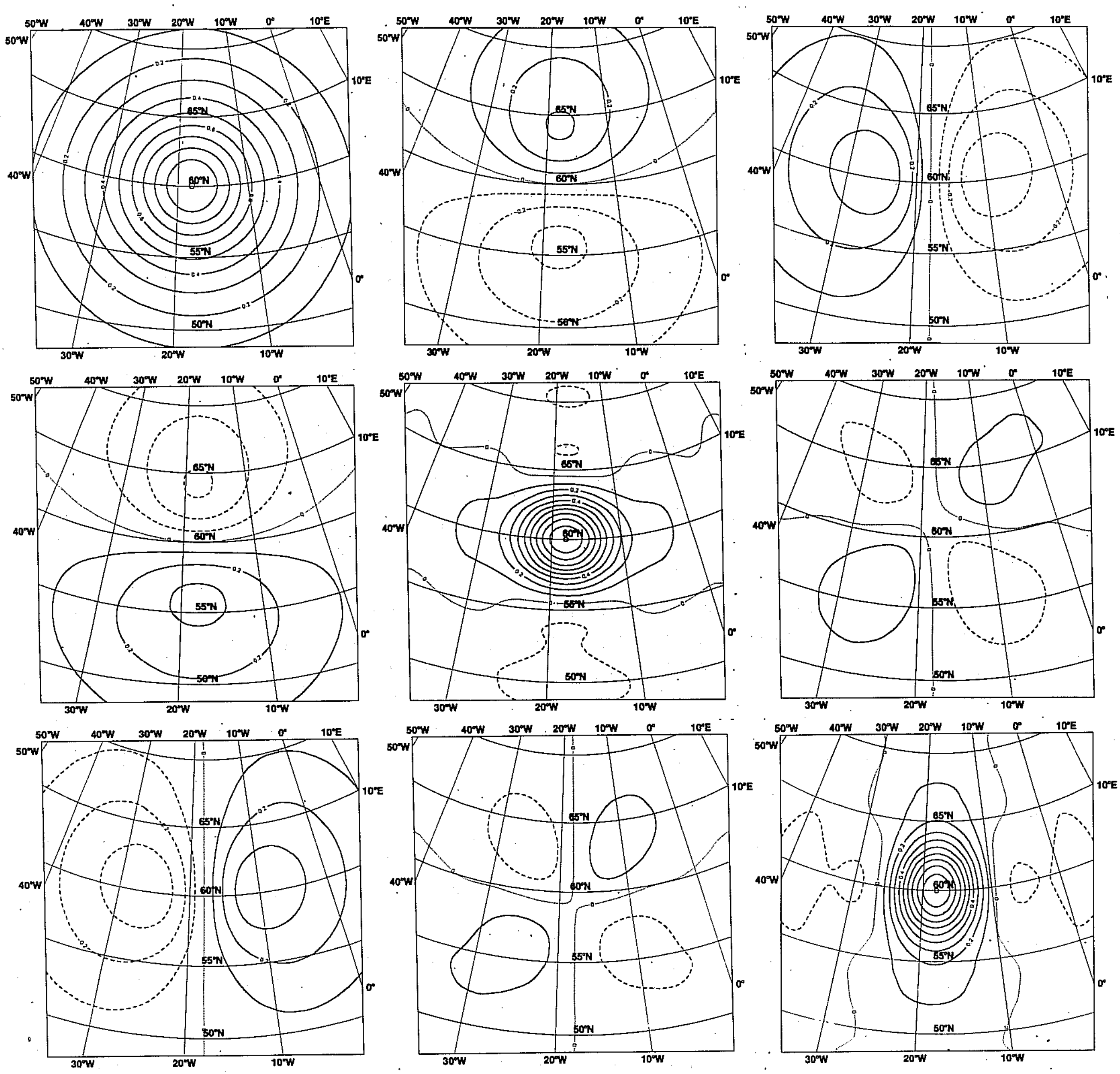

Fig.1 500 hPa 3D-Var structure functions at 60N. The first row depicts the z-z (left), z-u (middle) and z-v (right) correlations, the second row depicts the u-z (left), u-u (middle) and u-v (right) correlations, and the third row depicts the v-z (left), v-u (middle) and v-v (right) correlations.

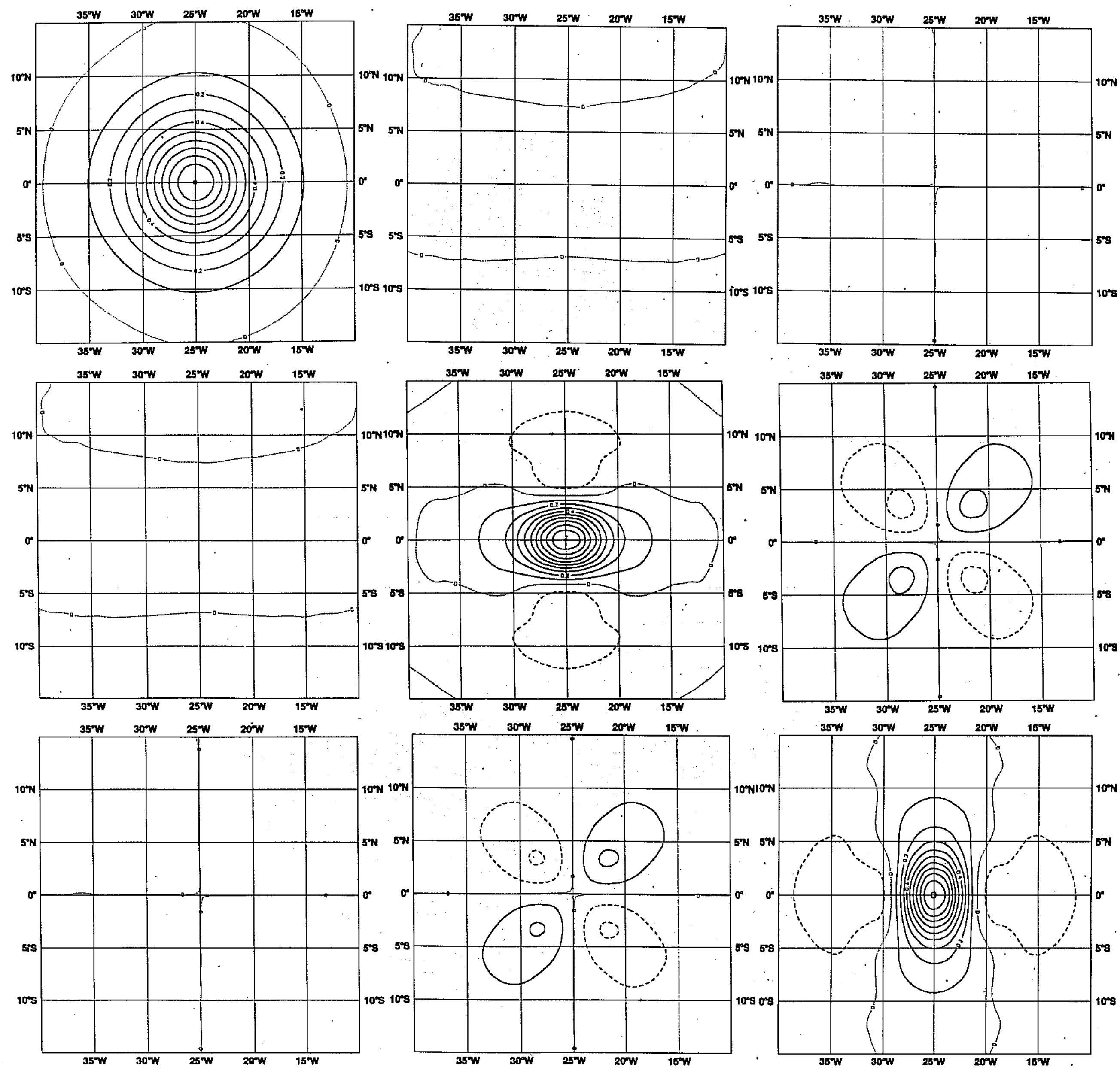

Fig.2 Same as Fig. 1. at the equator.

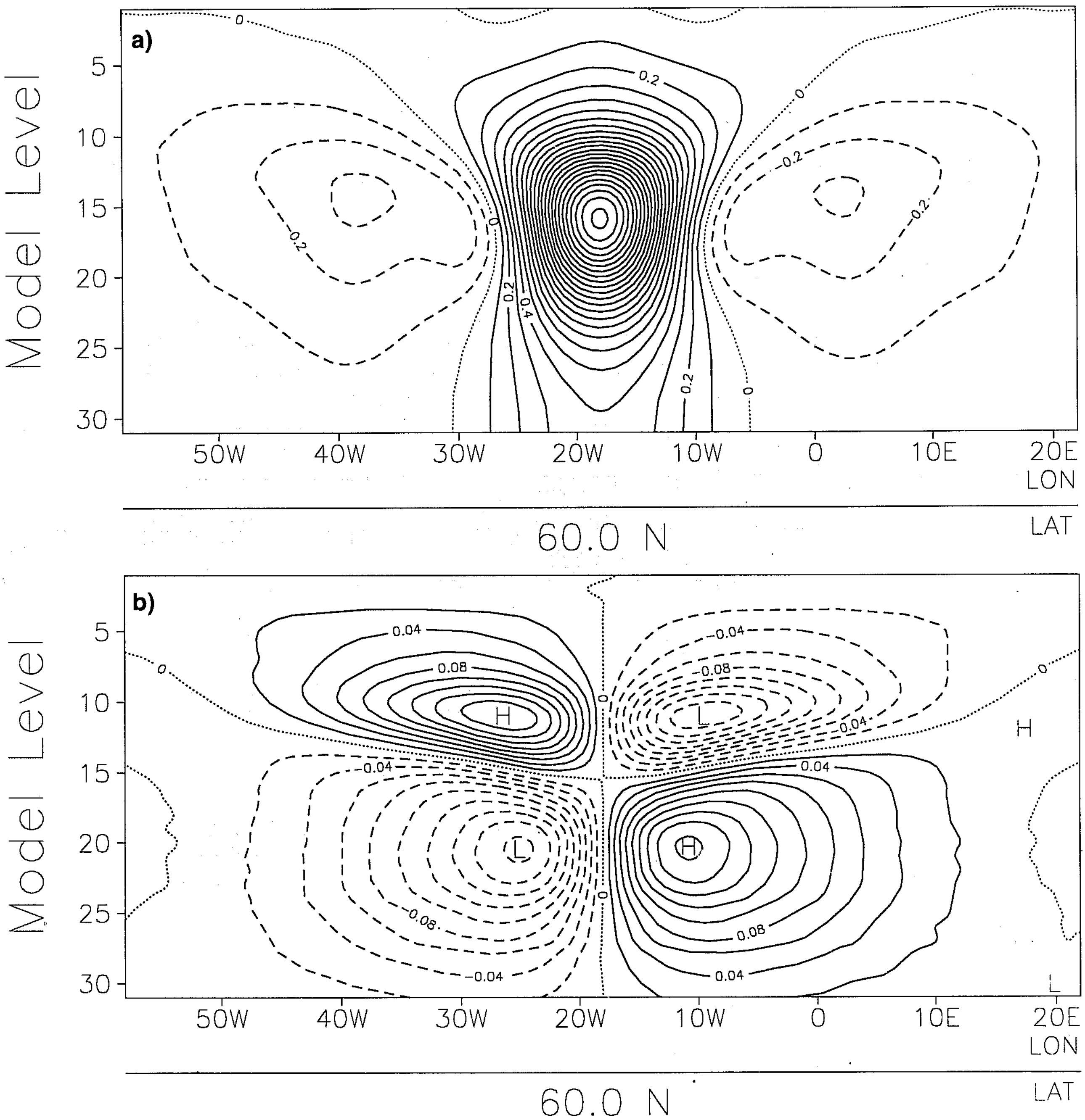

Fig.3 v-v (panel a) and v-T (panel b) covariances in a North-South vertical plane.